BAND STRUCTURE OF MoS$_2$ USING QUANTUM ESPRESSO

A PROJECT REPORT
Submitted by
AMRUTHA T
M MEENAKSHI
To
The MAHATMA GANDHI UNIVERSITY, KOTTAYAM

In partial fulfilment of the requirements for the award of
the Degree
Of
Bachelor of Science
In
Physics

Department of Physics
Bharata Mata College, Thrikkakara

DECLARATION

I undersigned hereby declare that the project report "**BAND STRUCTURE OF MoS$_2$ USING QUANTUM ESPRESSO**", submitted for partial fulfilment of the requirements for the award of degree of Physics of the Mahatma Gandhi University, Kerala is a bonafide work done by me under supervision of Anu Philip , Asst. Professor, Dept. Of Physics. This submission represents my ideas in my own words and where ideas or words of others have been included; I have adequately and accurately cited and referenced the original sources. I also declare that I have adhered to ethics of academic honesty and integrity and have not misrepresented or fabricated any data nor idea or fact or source in my submission. I understand that any violation of the above will be a cause for disciplinary action by the institute and/or the University and can also evoke penal action from the sources which have thus not been properly cited or from whom proper permission has not been obtained. This report has not been previously formed the basis for the award of any degree, diploma or similar title of any other University.

Place: Kochi

DEPARTMENT OF PHYSICS

BHARATA MATA COLLEGE THRIKKAKARA, KOCHI

CERTIFICATE

This is to certify that the report entitled BAND STRUCTURE OF MoS_2 USING QUANTUM ESPRESSO submitted by <u>AMRUTHA T AND M MEENAKSHI</u> to the Mahatma Gandhi University in partial fulfilment of the requirements for the award of the Degree of Bachelor of Science in Physics is a bonafide record of the project work carried out by him/her under my/our guidance and supervision. This report in any form has not been submitted to any other University or Institute for any purpose.

Internal Supervisor   External Supervisor

Head of the Department   Dr. Anu Philip
Physics   Assistant professor
Department of Physics

ACKNOWLEDGEMENT

Before getting into the thickest of things, we would like to thank the personalities who were part of our project in numerous ways, those who gave us outstanding support from the birth of the project. We are extremely thankful to Dr. ANU PHILIP, Assistant Professor of department Of Physics, for providing the necessary infrastructures and resources for the accomplishment of our project and for the esteemed guidance, moral support and invaluable provided by her for the success of the project at BHARATA MATA COLLEGE, KOCHI.

We are highly indebted to DR. JOHNSON K M, the principal of our college, for his support, during the tenure of the project. We are also thankful to all the staff members of the Physics department who have cooperated in making our project a success. We would like to thank all our parents and friends who extended their help, encouragement and moral support either directly or indirectly in our project work.

Thanks for your Valuable Guidance and support.

M. Meenakshi

Amrutha T

ABSTRACT

In this study, we explore the electronic band structure of molybdenum disulfide (MoS2), a prominent two-dimensional material, employing Quantum ESPRESSO, a widely-used package for electronic structure calculations based on density functional theory (DFT). MoS_2 has garnered significant attention due to its unique electronic, optical, and mechanical properties, rendering it promising for various applications in nanoelectronics, optoelectronics, and beyond. By utilizing Quantum ESPRESSO, we calculate the electronic band structure of MoS_2, which provides crucial insights into its fundamental electronic properties, such as the bandgap, band dispersion, and density of states. Our analysis elucidates the nature of electronic transitions and the presence of band gaps crucial for understanding its behavior in devices. Additionally, we investigate the impact of external perturbations, such as strain or doping, on the band structure, offering valuable guidance for tailoring MoS_2-based devices for specific applications. Overall, our study contributes to a deeper understanding of the electronic properties of MoS_2, facilitating its continued exploration and utilization in next-generation electronic and optoelectronic devices.

# CONTENT

CHAPTER 1

1.1 INTRODUCTION

Two-dimensional molybdenum disulfide (2D MoS_2) has emerged as a remarkable material with transformative properties and versatile applications in various fields of science and technology. Unlike its bulk counterpart, which exhibits an indirect bandgap, monolayer or few-layer MoS_2 possesses a direct bandgap, endowing it with exceptional optical and electronic properties. This unique characteristic makes 2D MoS_2 highly desirable for applications in optoelectronics, catalysis, sensing, and energy storage devices. Its atomically thin structure, coupled with strong quantum confinement effects, facilitates efficient charge carrier transport and manipulation at the nanoscale level. Additionally, the large surface-to-volume ratio of 2D MoS_2 enhances its reactivity and enables precise control over surface chemistry, making it an ideal candidate for catalytic and sensing applications. As research continues to unravel the diverse properties and potential applications of 2D MoS_2, its significance in advancing nanotechnology and contributing to innovations in various industries becomes increasingly evident.

1.2 MoS_2 - BACKGROUND INFORMATION

Molybdenum disulphide (MoS_2) is an inorganic material composed of 1 molybdenum and 2 sulphide. This chemical has a molar mass of 160.07 g/mol. The substance is categorised as a dichalcogenide of transition metals. The silvery-black solid mineral molybdenite is the primary source of molybdenum. MoS_2 is not very reactive. Oxygen and diluted acids have no effect on it. Graphite and molybdenum disulfide are similar in appearance and feel. Due to its resilience and low friction, it finds extensive application as a dry lubricant. With a bandgap of 1.23 eV, bulk MoS_2 is a diamagnetic, indirect bandgap semiconductor related to silicon.

MoS$_2$ can be found in nature as either the crystalline mineral molybdenite or the uncommon low-temperature variant of molybdenite called jordisite.Flotation is used to separate the comparatively pure MoS$_2$ from molybdenite ore. Carbon is the primary contaminant. In addition, almost all molybdenum compounds can be thermally treated with hydrogen sulphide or elemental sulphur to form MoS$_2$, which can also be created through metathesis events from molybdenum pentachloride.
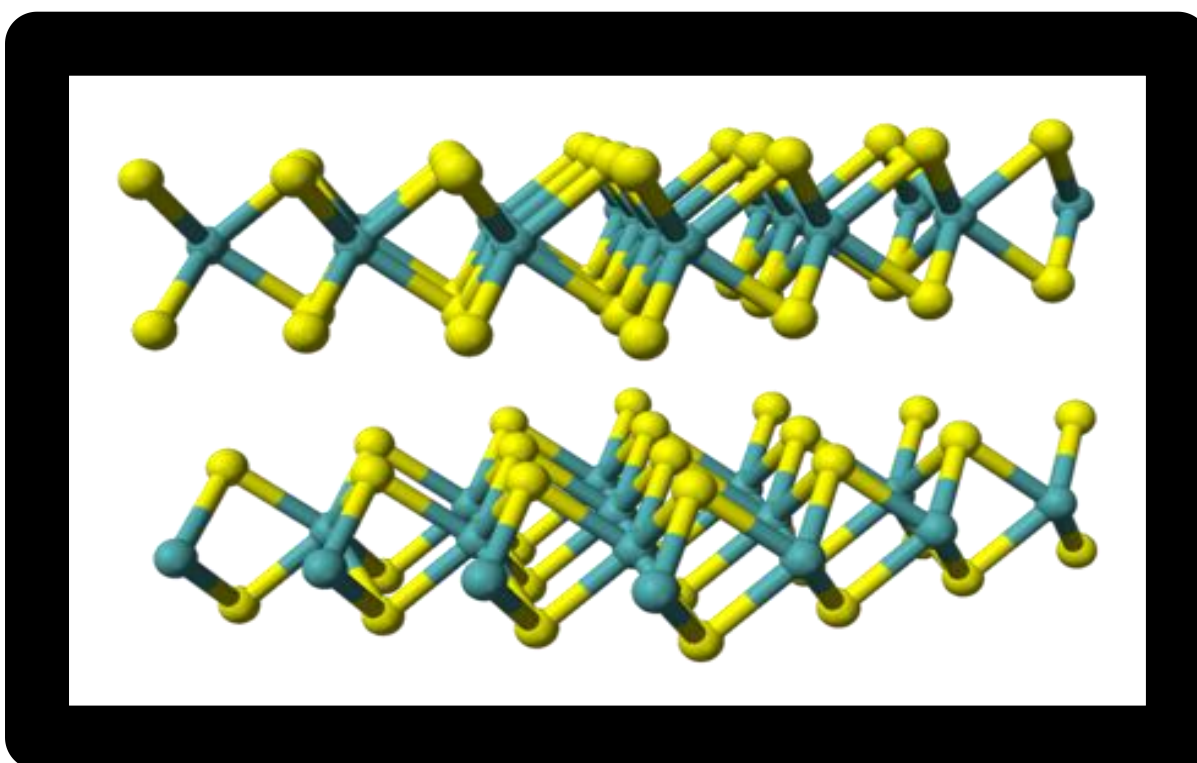
Every form of MoS_2 is composed of layers, with sulphide ion planes encircling a plane of molybdenum atoms. These three layers combine to form a MoS_2 monolayer. Weak van der Waals interactions hold stacked monolayers that make up bulk MoS_2 together.

The names 2H-MoS_2 and 3R-MoS_2, respectively, refer to two different phases of crystalline MoS_2, where the "H" and "R" stand for hexagonal and rhombohedral symmetry. Each molybdenum atom in each of these complexes is covalently bonded to six sulphide ions and is situated at the centre of a trigonal prismatic coordination sphere. Each sulphur atom is coupled to three molybdenum atoms and exhibits pyramidal coordination. The 3R-phase and the 2H-phase are both semiconducting.

Intercalating alkali metals with 2H-MoS_2 resulted in the discovery of a third, metastable crystalline phase called 1T-MoS_2.This phase is metallic and possesses trigonal symmetry. The 1T-phase can be returned to the 2H-phase by microwave radiation or stabilised by doping with electron donors such as rhenium. By adding S vacancies, the 2H/1T-phase transition can be regulated.

MoS2, with the chemical formula MX2, belongs to the class of layered 2D transition metal dichalcogenides (TMDCs)[1]. The transition metal element is denoted by M, and S, Se, or Te are represented by X. The stacking of X-M-X layers creates the bulk TMDCs, which can exist in varying structural stages based on the atoms of the transitional metal. Mo (+4) and S (−2) are placed in a S–Mo–S configuration in single-layered MoS2 films, with six S atoms surrounding one Mo atom in each layer. MoS2 often appears in two structural phases: octahedral (1T) or trigonal prismatic (2H/3R). The stacking arrangement of layers in MoS2 with regard to Mo coordination determines the structural phases. With the ABA layer stacking, the 2H structure is the predominant stable phase seen in nature.It features two layers with hexagonal symmetry arranged in each unit cell. In this instance, the sulfur atoms from various atomic planes are perpendicular to one another and occupy the same locations. While the S layers are easily able to glide against one other and are connected by van der Waals interactions, the Mo–S connection is primarily covalent.

This structural property helps to cleave crystals along with the surface layers (Z direction) by breaking weak van der Waals forces, and this property is exploited in the synthesis of single-layered MoS_2
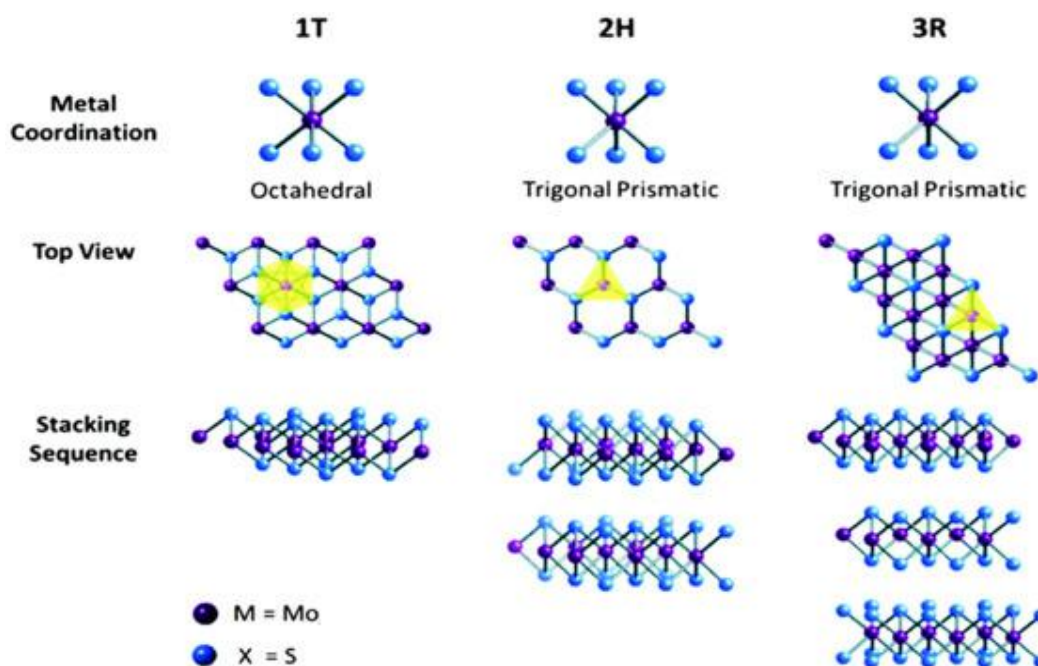
When MoS$_2$ is synthesised, it often exhibits a 3R structure, which is very unstable and has three layers per unit cell and a rhombohedral symmetry. When heated, this structure's orientation can be changed to a 2H type. The Mo hexagonal arrays are positioned between the sulphur layers in the 2H and 3R MoS$_2$ structures. One of the sulphur layers in MoS$_2$ is disoriented to produce the 1T crystal structure, which has an ABC layering sequence. It possesses a trigonal symmetry, or the metallic 1T phase, and a symmetrical Mo–Mo bond. MoS$_2$ exhibits varying electrical conductivity depending on its phase and crystal structure. Since 1T phases contain more exposed active sites, their presence increases the MoS$_2$'s electrical conductivity.

From two-dimensional (2D) sheets of MoS$_2$ to their three-dimensional (3D) bulk equivalent, the material's band structure varies.

The physical and chemical characteristics of MoS$_2$ are determined by the number of layers present in the material. While the monolayer MoS$_2$ has an indirect bandgap of 1.9 eV, the bulk MoS$_2$ displays a direct bandgap of 1.3 eV. Quantum confinement, interlayer interactions, and long-range Coulomb effects are possible contributors to this phenomena.

In the case of the bulk counterpart, an indirect bandgap is shown between the conduction band (CB) lowest point, K (Brillouin zone point), and the γ (gamma), valence band (VB) maximum point. The CB and VB edges in the illustration are shown by the red and blue lines, respectively. The molybdenum d-orbitals attribute to

the K value, and as this value is independent of the number of layers, it will not alter as the size lowers. Sulphur's 2p orbitals make up the VB. Because it is made up of hybridised orbitals of pz and d orbitals of S and Mo, respectively, the bandgap between K and γ changes as a result. With a decreasing number of layers, the VB maximum (VBM) point γ falls below zero to create a fresh VBM point. The monolayer's lowest energy transition is vertical, or direct, and the energy required for the monolayer's indirect transition is more than that required for the direct band edge transition. There will be an enlarged gap of 1.9 eV in the newly developed band gap between the new γ and the stable K point.
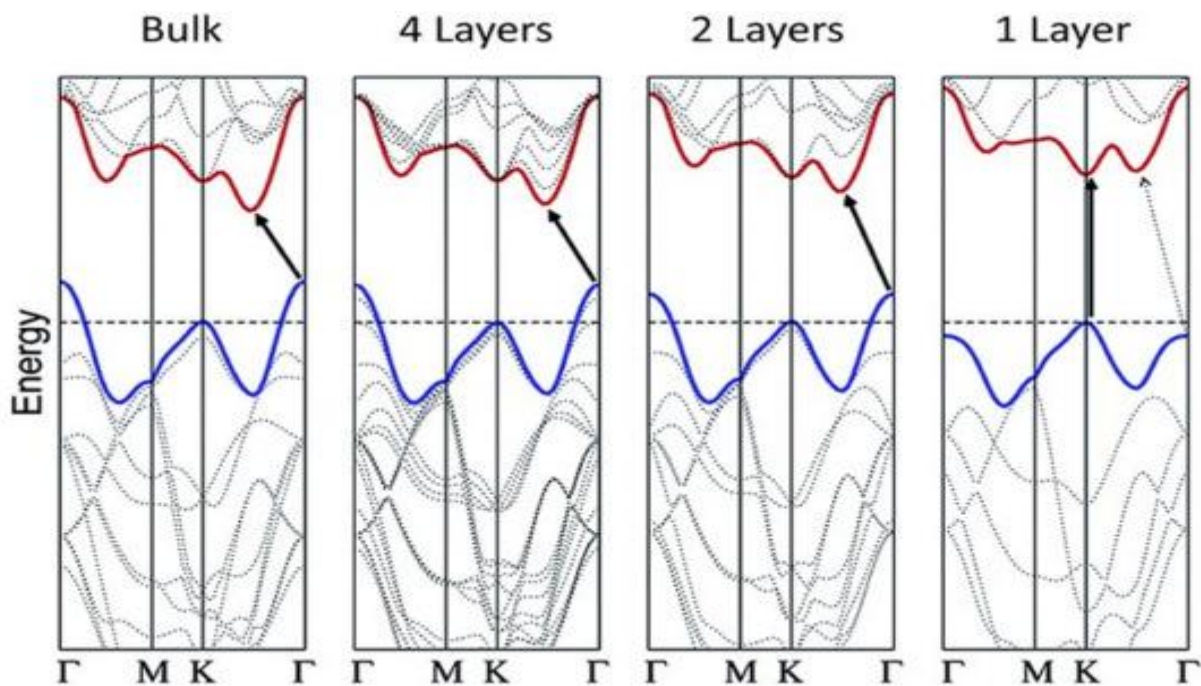
1.3 Key Characteristics and Diverse Applications of Two-Dimensional Molybdenum Disulfide (MoS$_2$)

● Layered Structure: MoS$_2$ is a two-dimensional substance that resembles graphene in its layered structure. Its structure confers special mechanical, optical, and electrical qualities.

● Semiconducting Characteristics: MoS$_2$ is a semiconductor with a large bandgap, in contrast to graphene, which has a zero bandgap. Because of this characteristic, it may be used in optoelectronic devices, integrated circuits, and transistor applications in electronics.

● High Carrier Mobility: MoS_2 demonstrates a critical quality for effective electronic devices: high charge carrier mobility. Because of its great mobility, it can be quickly charged and is hence appropriate for high-speed electronics.

● Tunable Bandgap: MoS_2's band gap may be adjusted for a variety of optoelectronic and electrical applications by varying its thickness or applying strain.

● Chemical Stability: Unlike many other 2D materials that are prone to oxidation, MoS_2 is chemically stable, especially under ambient circumstances. Its usefulness for real-world applications is improved by this steadiness.

● Huge Surface Area: MoS_2's enormous surface area is a benefit for applications like energy storage, sensing, and catalysis because of its 2-dimensional (2D) structure.

● Biocompatibility: Because of MoS_2's low toxicity and biocompatibility, it has demonstrated potential in biomedical applications. It can be used for imaging agents, biosensors, and medication delivery systems.

● MoS_2's optical features are intriguing and include high photoluminescence and nonlinear optical activity. As a result, it may be used in photovoltaic systems, light-emitting diodes (LEDs), and photodetectors.

● Thermal Conductivity: MoS_2 has a somewhat high thermal conductivity, however not as high as graphene. This is useful for heat management applications in electronics.

● Low Cost and Abundance: The ingredients that make up MoS_2, sulphur and molybdenum, are inexpensive and abundant when compared to some other 2D materials. This can make large-scale manufacture more financially feasible.

2D MoS_2 exhibits versatile applications due to its absorption spectrum falling within the visible electromagnetic range. Reports indicate its utilization in diverse fields such as energy storage, hydrogen generation, pollutant degradation, and disinfection. Recent studies have extensively documented MoS_2's photocatalytic properties across various application domains.

1.4 OVERVIEW OF BAND STRUCTURE AND THEIR SIGNIFICANCE IN ELECTRICAL PROPERTIES

Band structure calculations are pivotal in elucidating the electronic properties of materials, offering crucial insights into their behaviour and functionalities. By examining the band structure, which depicts the distribution of energy levels for electrons within a material, The band structure reveals critical information such as the presence of energy bands, band gaps, and band dispersions, all of which are instrumental in determining the material's conductivity, optical properties, and electronic behaviour. For instance, the presence of a band gap indicates whether a material is an insulator, semiconductor, or metal, thereby defining its electrical conductivity

1.4.1 BAND GAP

A band gap, also known as an energy gap or bandgap in solid-state physics, is an energy range in a solid when no electronic states are present. On graphs of the electrical band structure of solids, the term "band gap" refers to the energy difference (usually expressed in electron volts) between the top of the valence band and the bottom of the conduction band in insulators and semiconductors.

To move an electron from the valence band to the conduction band, energy is needed. In order to carry electric current, the resultant conduction-band electron (as well as the electron hole in the valence band) are free to move inside the crystal lattice.Each type of solid has a unique energy-band structure. The vast diversity of electrical properties seen in different materials can be attributed to this variance in band structure. The spectroscopy and band structure can change depending on the dimension. The valence and conduction bands overlap in conductors. This overlap allows the valence electrons to almost freely enter the conduction band and participate in conduction. A portion of the valence electrons

can only pass through the material because of the partial overlap, but this is still sufficient to make conductors conductive.

The gap in semiconductors is small enough to be filled by an excitation of some kind, maybe solar radiation in the case of photovoltaic cells. In essence, the gap is a distance "in-between" an insulator and a conductor.
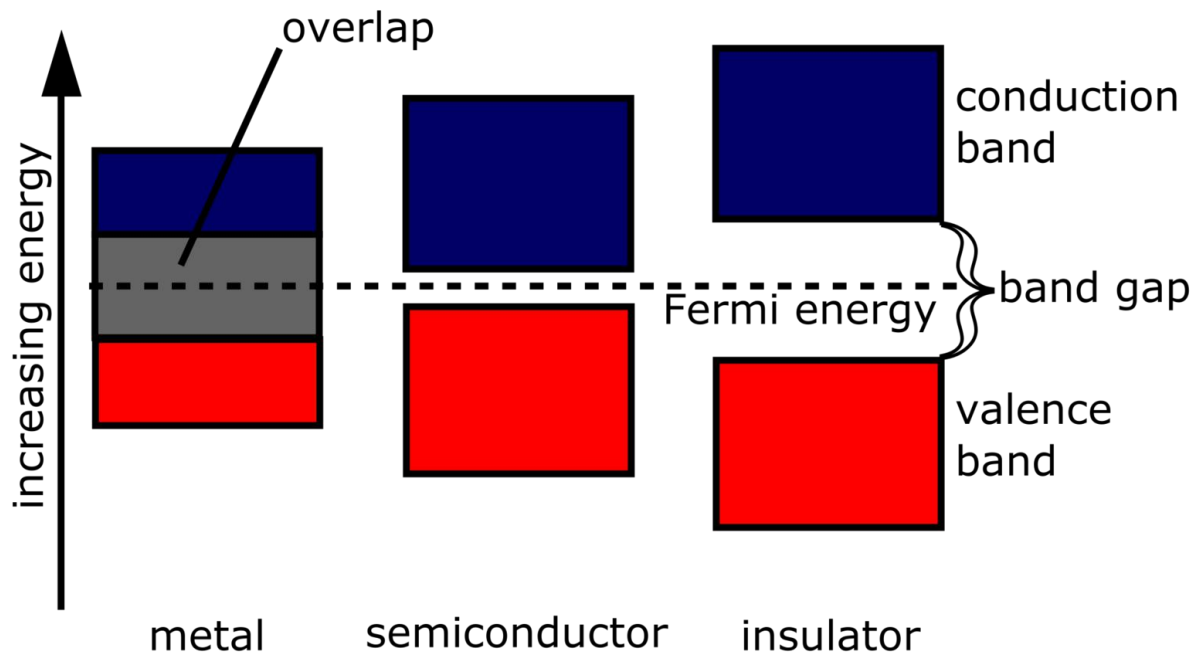
A semiconductor's band gap can be classified as either an indirect or direct band gap. A certain crystal momentum (k-vector) in the Brillouin zone characterises the minimal-energy state in the conduction band and the maximal-energy state in the valence band, respectively. The material has an "indirect gap", if the k-vectors disagree.

When electrons and holes have the same crystal momentum in both the valence band and the conduction band, the band gap is referred to as "direct" because an
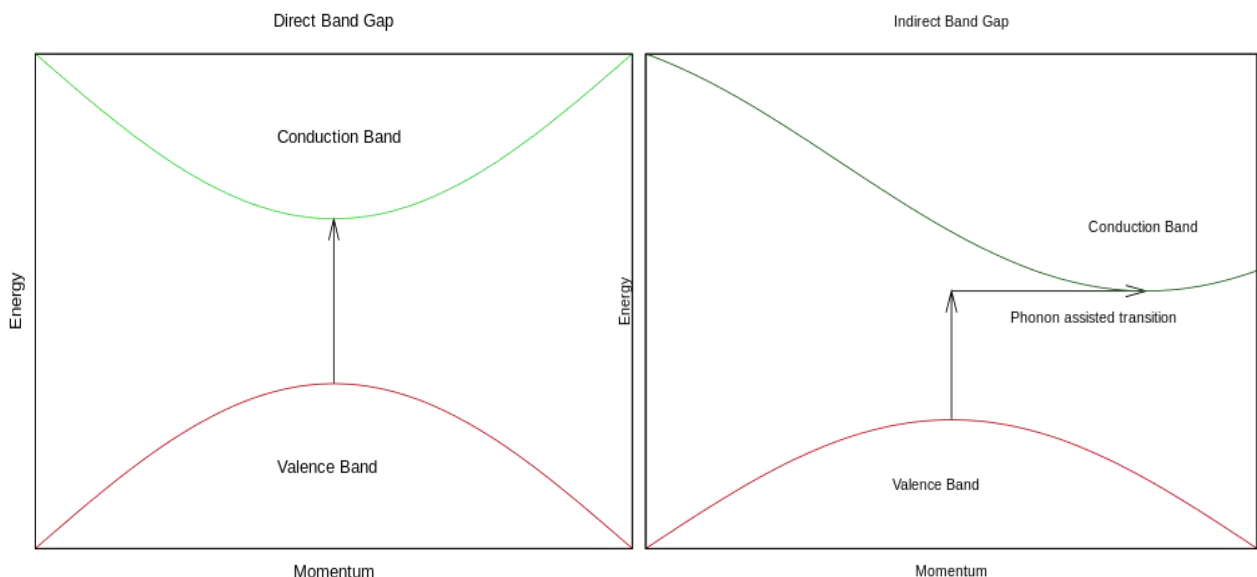
electron can emit a photon directly. Since the electron needs to transmit momentum to the crystal lattice through an intermediary state, a photon cannot be released in an "indirect" gap.

Formula for finding direct and indirect band gap of a crystal structure

$$\alpha \propto (h\nu - E_g \pm E_p)^2 \qquad \text{in indirect band gap}$$

$$\alpha \propto (h\nu - E_g)^{\frac{1}{2}} \qquad \text{in direct band gap}$$

Where alpha is the absorption; h is planck's constant; v is the frequency; E is the energy of the band gap

1.5 OBJECTIVES

Various software options are available for analysing and computing the electronic structure and associated parameters of a system. The primary objective of this project is to investigate the bandgap structure and determine the bandgap energy of MoS_2 using Density Functional Theory (DFT) implemented in Quantum Espresso. Initially, the MoS_2 structure is manipulated to meet the necessary conditions for obtaining the band structure. Subsequently, the bandgap energy is calculated from the resulting band structure graphically. This calculated bandgap energy is then compared with theoretically obtained values to assess accuracy. The MoS2 structure is sourced from the Computational 2D Material Database (C2DB), which hosts over 40 unique crystal structures encompassing various properties of nearly 4000 two-dimensional (2D) materials, including structural, thermodynamic, elastic, electrical, magnetic, and optical properties. Density Functional Theory (DFT) and many-body perturbation theory are employed for computational analysis. Through this investigation, the project aims to contribute to the understanding of MoS_2's electronic properties and their potential applications in material science and related fields.

CHAPTER 2

2.1. DENSITY FUNCTION THEORY(DFT)

Density Functional Theory (DFT) revolutionizes material science by providing a robust computational framework for analyzing the electronic properties of materials. At its core, DFT relies on the concept of electron density, representing the spatial distribution of electrons within a material. By solving the Schrödinger equation for electron density, DFT allows researchers to compute critical parameters like total energy, charge density, and wave functions.

DFT finds widespread application in computing band structures, which delineate the distribution of energy levels for electrons in materials. This information offers insights into electrical conductivity and optical properties, facilitating the design of electronic devices and semiconductor materials. Additionally, DFT aids in determining the total energy of materials, crucial for understanding stability, bonding, and phase transitions. By optimizing atomic structures based on total energy minimization, researchers gain valuable insights into material stability and reactivity, with implications for catalysis and materials design.

Furthermore, DFT provides electronic charge density distributions, unveiling details about chemical bonding and inter atomic interactions. By analyzing charge density, researchers discern bonding and non-bonding regions within materials, informing on their chemical and physical properties. Overall, DFT serves as an indispensable tool in materials science, enabling the prediction and understanding of electronic properties in various materials, from semiconductors to metals and insulators. Its versatility and predictive capabilities make DFT instrumental in accelerating materials discovery and advancing applications in fields such as electronics, catalysis, and energy storage

Density Functional Theory (DFT) calculations are instrumental in predicting the electronic properties of materials, offering insights into band structures, DFT computations enable the determination of the electronic band structure of materials. By solving the Kohn-Sham equations within DFT, which describe the behavior of electrons in a material's periodic lattice potential, the energy eigenvalues and corresponding wave functions of electrons are obtained. These results reveal the distribution of energy levels (bands) for electrons in the material, providing critical information about its electronic properties. Band structures elucidate phenomena such as electrical conductivity, optical absorption, and the formation of energy bands and band gaps, which are crucial for understanding and designing electronic and opt-electronic devices.

2.2. QUANTUM ESPRESSO

Quantum Espresso is a set of free software available under the GNU General Public Licence that is used for first-principles electronic-structure computations and materials modelling. Density-functional theory (DFT) is its foundation.

An atom, molecule, or condensed phase can be modeled using density-functional theory (DFT), a computational quantum mechanical model used in physics, chemistry, and materials science to investigate the electronic structure (or nuclear structure) of many-body systems (primarily the ground state).With this theory, many-electron systems can be determined by using functionals, i.e. functions of other functions.DFT uses spatially dependent electron densities as functionals.Condensed-matter physics, computational physics, and computational chemistry use DFT as one of their most popular and versatile methods.Solid-state physics has made extensive use of DFT for calculations.Computational materials science utilizes DFT calculations to predict and calculate material behaviour using quantum mechanical considerations, without requiring higher-order parameters like fundamental material properties. A potential acting on the electrons of the system is used in contemporary DFT techniques to evaluate electronic structure.

Hence, Density functional theory is generally used more and more in chemistry and materials science to explain and forecast the behaviour of complex

systems at the atomic scale. DFT computational techniques are specifically used for systems and processing parameters relevant to synthesis. Experimental research in such systems is frequently hindered by non-equilibrium conditions and conflicting results.

Studying the effects of dopants on phase transformation behaviour in oxides, magnetic behaviour in materials containing diluted magnetic semiconductors, and the investigation of magnetic and electronic behaviour in ferroelectrics and dilute magnetic semiconductors are a few examples of modern DFT applications.

BURAI is a GUI system of Quantum ESPRESSO. It is a JavaFX application that allows you to use Quantum ESPRESSO, a powerful and versatile electronic-structure simulation package, in a graphical user interface.
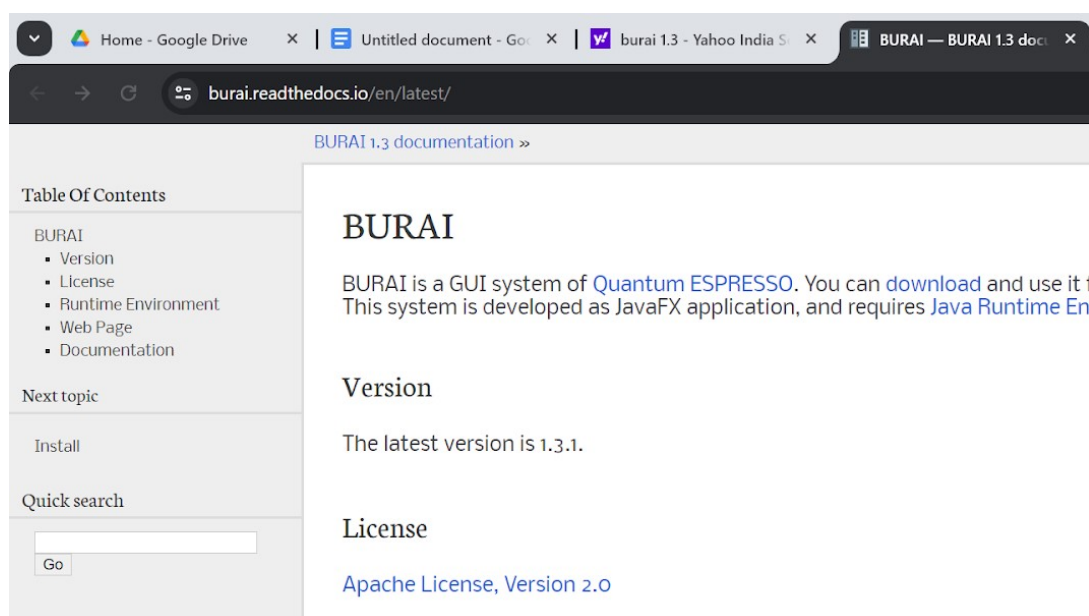
CHAPTER 3
CALCULATION SETUP

3.1. INSTALLING BURAI

STEP 1- Go to 'https://burai.readthedocs.io/en/latest/' .

STEP 2- install the latest version of Burai i.e. Burai 1.3.1.

STEP 3- If the application depends on the other compressed files in the folder then extract all the files at desired place.

STEP 4- After extracting, run the application. Burai is all set to use.

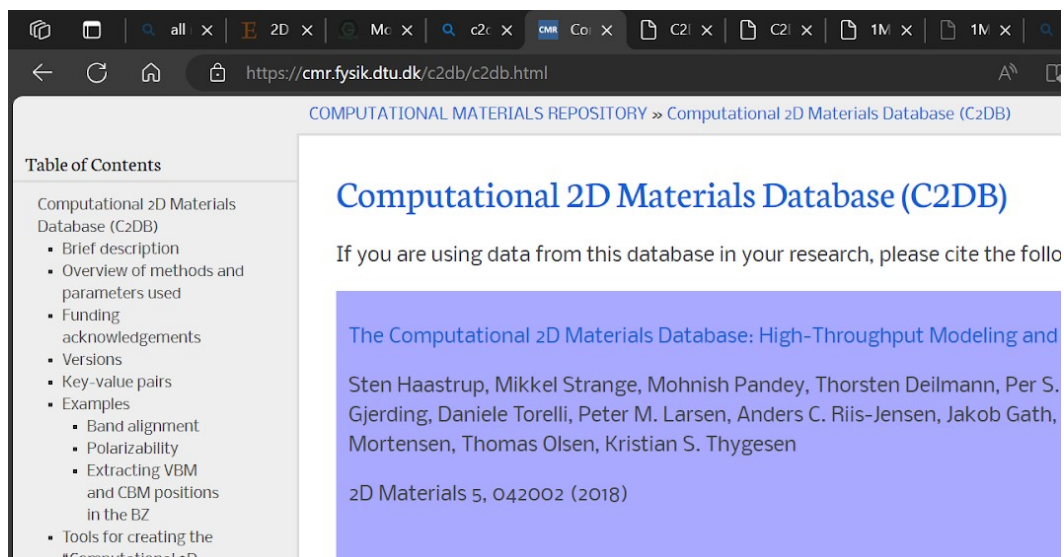## 3.2. IMPORTING THE COMPOUND FROM C2DB(Computational 2D Materials Database)

STEP 1- Go to 'Computational 2D Materials Database (C2DB) — COMPUTATIONAL MATERIALS REPOSITORY (dtu.dk)'.

STEP 2- Go to browse data and search for MOS2.

STEP 3- Select the desired structure from the options.

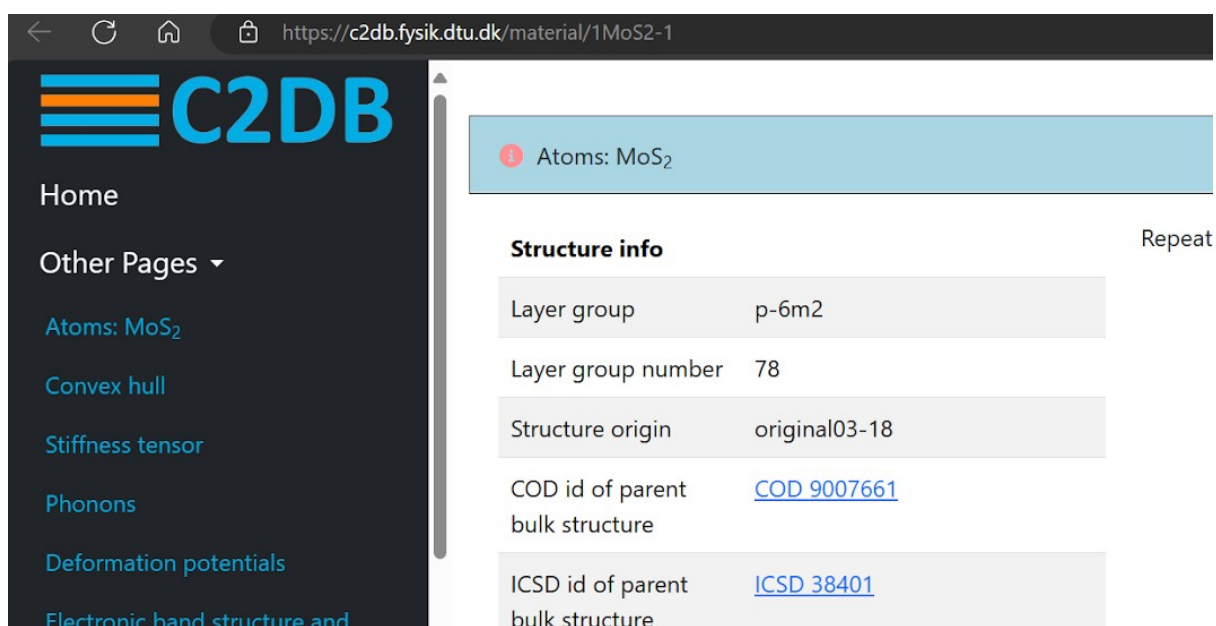STEP 4- Download the CIF/XYZ file format of the structure of MoS2.

STEP 5- Import the file into the Burai interface.

3.3.OBTAINING THE BAND STRUCTURE AND CALCULATING THE BANDGAP ENERGY

STEP 1- Suitable/required changes are made in the 2D structure of MoS_2 and hence the input file is set up.

STEP 2- The structure is saved and run i.e, the calculation of the band takes place.

STEP 3- After the calculation is done, the structure output (i.e. the band structure) is obtained under the result tag.

STEP 4- The band gap energy is calculated by observing the gap between the lowest conduction band and highest valence band which gives the band gap energy of the structure.

>

1 × bandmos2 ×

Input-file   ↑ ↺ ✕

```
        startingwfc       = "atomic+random"
/

&DOS
    degauss =  1.00000e-02
    deltae  =  1.00000e-02
    emax    =  1.50000e+01
    emin    = -1.50000e+01
    ngauss  = 0
/

&PROJWFC
    degauss =  1.00000e-02
    deltae  =  1.00000e-02
    emax    =  1.50000e+01
    emin    = -1.50000e+01
    ngauss  = 0
/

K_POINTS {automatic}
 9  9  1  0 0 0
```

>

1 ×

Band structure
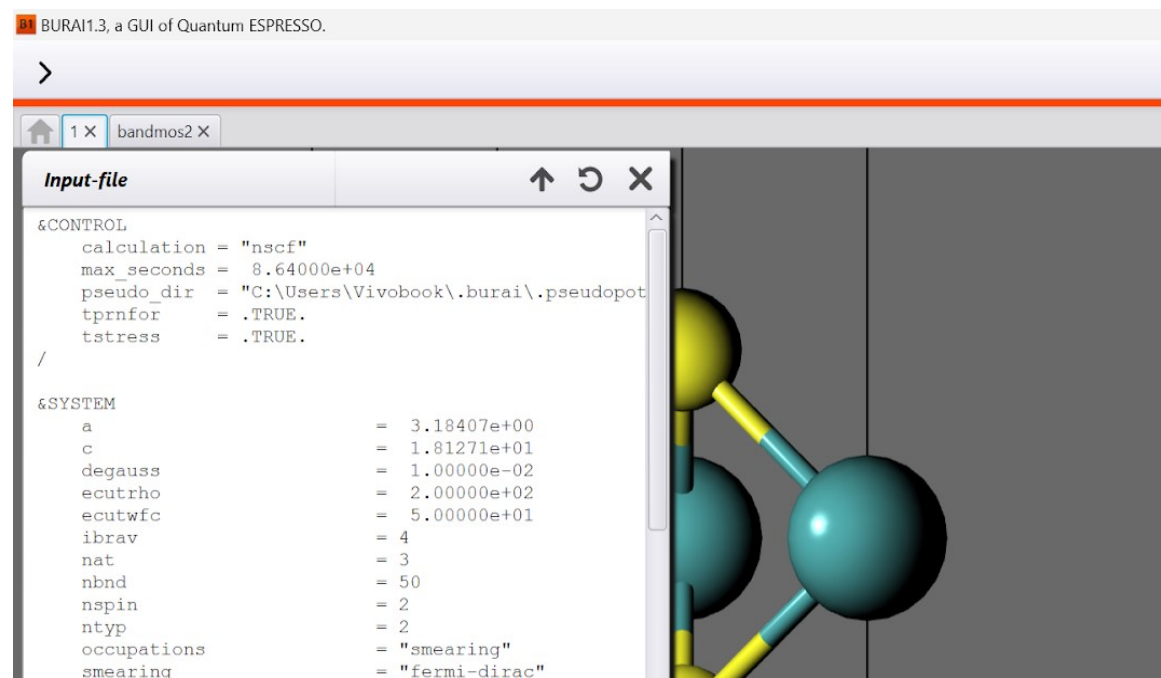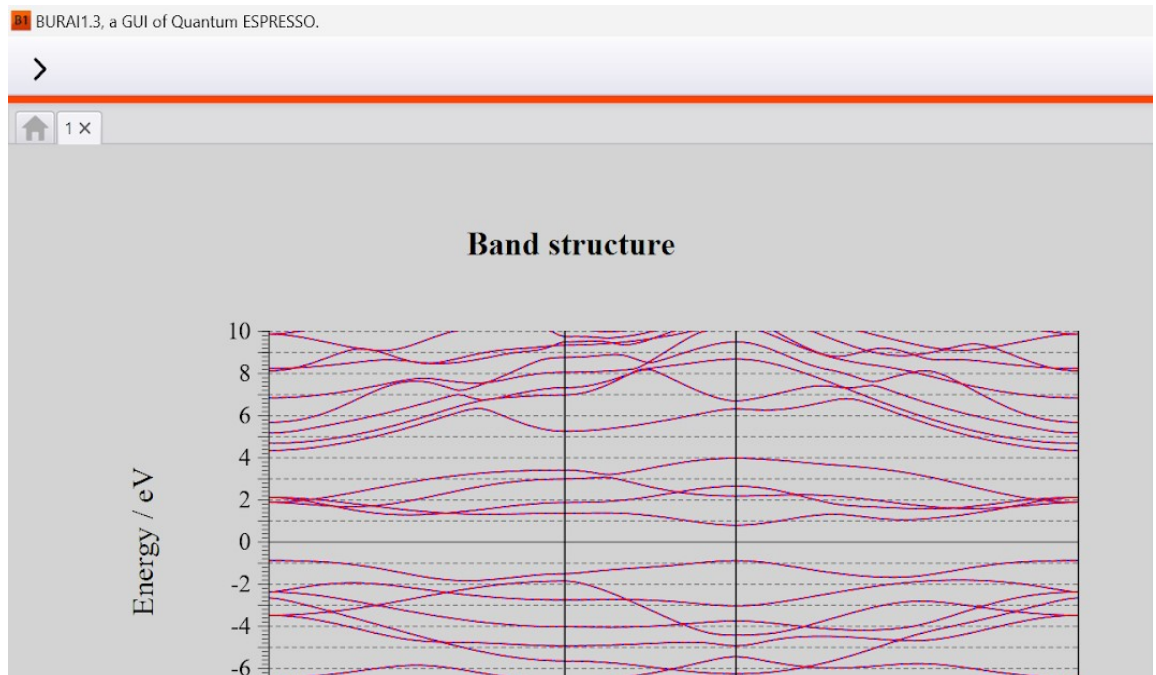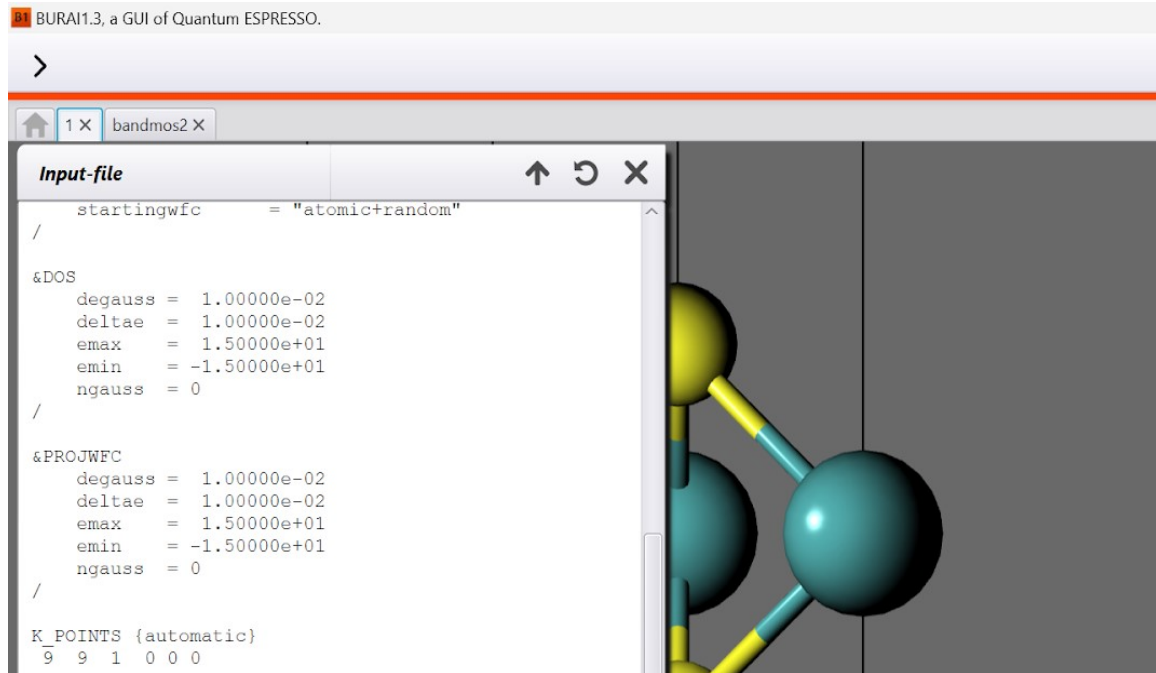
3.4. INPUT (DOS PROPERTIES)

```
&CONTROL
  calculation = "bands"
  max_seconds =   8.64000e+04
```

```
    outdir      = "./"
    prefix      = "espresso"
    pseudo_dir  = "C:\Users\Vivobook\.burai\.pseudopot"
    title       = "1(Band)"
    tprnfor     = .TRUE.
    tstress     = .TRUE.
    wf_collect  = .TRUE.
    wfcdir      = "./"
/

&SYSTEM
    a                       =  3.18407e+00
    c                       =  1.81271e+01
    degauss                 =  1.00000e-02
    ecutrho                 =  2.00000e+02
    ecutwfc                 =  5.00000e+01
    ibrav                   = 4
    nat                     = 3
    nbnd                    = 50
    nspin                   = 2
    ntyp                    = 2
    occupations             = "smearing"
    smearing                = "fermi-dirac"
    starting_magnetization(1) =  2.00000e-01
    starting_magnetization(2) =  0.00000e+00
/


&ELECTRONS
    conv_thr           =  1.00000e-06
    electron_maxstep = 200
    mixing_beta        =  4.00000e-01
    startingpot        = "atomic"
    startingwfc        = "atomic+random"
/

&BANDS
    filband         = "espresso.band2"
    lsym            = .FALSE.
    outdir          = "./"
    prefix          = "espresso"
    spin_component = 2
/

K_POINTS {tpiba_b}
4
gG     50
M      50
K      50
gG     50
```

```
ATOMIC_SPECIES
Mo      95.94000   Mo.pbe-spn-rrkjus_psl.1.0.0.UPF
S       32.06600   S.pbe-van_bm.UPF

ATOMIC_POSITIONS {angstrom}
Mo      0.000000   0.000000   9.063556
S       1.592033   0.919161  10.627113
S       1.592033   0.919161   7.500000
```

3.4.1.OPTIMIZATION OF MoS$_2$

Title:

1(Optimize)

```
bravais-lattice index      =            4
lattice parameter (alat)  =        6.0170  a.u.
unit-cell volume          =     1074.0408 (a.u.)^3
number of atoms/cell       =            3
number of atomic types     =            2
number of electrons        =        26.00
number of Kohn-Sham states=            17
kinetic-energy cutoff      =        50.0000  Ry
charge density cutoff      =        200.0000  Ry
convergence threshold      =        1.0E-06
mixing beta                =        0.4000
number of iterations used =            8   plain      mixing
Exchange-correlation      =  SLA  PW    PBE  PBE ( 1  4  3  4 0 0)
nstep                      =            201


celldm(1)=   6.017020  celldm(2)=   0.000000  celldm(3)=   5.693060
celldm(4)=   0.000000  celldm(5)=   0.000000  celldm(6)=   0.000000


crystal axes: (cart. coord. in units of alat)
        a(1) = (   1.000000    0.000000    0.000000 )
```

a(2) = (-0.500000   0.866025   0.000000)

                a(3) = (0.000000   0.000000   5.693060)

    reciprocal axes: (cart. coord. in units 2 pi/alat)

                b(1) = (1.000000   0.577350 -0.000000)

                b(2) = (0.000000   1.154701   0.000000)

                b(3) = (0.000000 -0.000000   0.175652)

    PseudoPot. # 1 for Mo read from file:

    C:\Users\Vivobook\.burai\.pseudopot/Mo.pbe-spn-rrkjus_psl.1.0.0.UPF

    MD5 check sum: 5b1023c46552c035e06f08f64a8d82ee

    Pseudo is Ultrasoft + core correction, Zval = 14.0

    Generated using "atomic" code by A. Dal Corso   v.5.1.2

    Using radial grid of 1229 points,   6 beta functions with:

                l(1) =   0

                l(2) =   0

                l(3) =   1

                l(4) =   1

                l(5) =   2

                l(6) =   2

    Q(r) pseudized with 0 coefficients

    PseudoPot. # 2 for S   read from file:

    C:\Users\Vivobook\.burai\.pseudopot/S.pbe-van_bm.UPF

    MD5 check sum: 5981569f150ce26f656387b858196b6a

    Pseudo is Ultrasoft, Zval =   6.0

    Generated by new atomic code, or converted to UPF format

  Using radial grid of   811 points,   6 beta functions with:

                l(1) =   0

                l(2) =   0

                l(3) =   1

                l(4) =   1

l(5) =   2

            l(6) =   2

   Q(r) pseudized with 8 coefficients, rinner =   1.100   1.100   1.100

                                                      1.100   1.100

   atomic species   valence   mass   pseudopotential

     Mo   14.00   95.94000   Mo(1.00)

     S   6.00   32.06600   S (1.00)

   Starting magnetic structure

   atomic species   magnetization

     Mo   0.200

     S   0.000

   12 Sym. Ops. (no inversion) found

  Cartesian axes

    site n.   atom   positions (alat units)

     1   Mo tau(1) = (0.0000000   0.0000000   2.8465316)

     2   S   tau(2) = (0.4999994   0.2886749   3.3375877)

     3   S   tau(3) = (0.4999994   0.2886749   2.3554759)

 number of k points=   4 Fermi-Dirac smearing, width (Ry)= 0.0100

              cart. coord. in units 2pi/alat

     k(1) = (0.0000000   0.0000000   0.0000000), wk =   0.0625000

     k(2) = (0.0000000   0.2886751   0.0000000), wk =   0.3750000

     k(3) = (0.0000000 -0.5773503   0.0000000), wk =   0.1875000

     k(4) = (0.2500000   0.4330127   0.0000000), wk =   0.3750000

   Dense grid: 51365 G-vectors   FFT dimensions: (27, 27, 160)

Estimated max dynamical RAM per process >   20.92MB

Estimated total allocated dynamical RAM >   83.70MB
Generating pointlists ...
new r_m :   0.3126 (alat units) 1.8812 (a.u.) for type   1
new r_m :   0.3126 (alat units) 1.8812 (a.u.) for type   2

Check: negative/imaginary core charge=   -0.000002   0.000000

Initial potential from superposition of free atoms

starting charge   25.99906, renormalised to   26.00000

negative rho (up, down):   9.979E-05 7.607E-05
Starting wfc are   18 randomized atomic wfcs

total cpu time spent up to now is   5.2 secs

Self-consistent Calculation

iteration #   1   ecut=   50.00 Ry   beta=0.40
Davidson diagonalization with overlap
ethr =   1.00E-02,   avg # of iterations =   2.5

Threshold (ethr) on eigenvalues was too large:
Diagonalizing with lowered threshold

Davidson diagonalization with overlap
ethr =   6.31E-04,   avg # of iterations =   1.2

negative rho (up, down):   1.008E-04 8.578E-05

total cpu time spent up to now is   12.1 secs

total energy   =   -180.60534820 Ry
Harris-Foulkes estimate   =   -180.61445141 Ry
estimated scf accuracy   <   0.16593173 Ry

total magnetization   =   0.02 Bohr mag/cell
absolute magnetization   =   0.78 Bohr mag/cell

iteration # 2   ecut=   50.00 Ry   beta=0.40
Davidson diagonalization with overlap
ethr =   6.38E-04,   avg # of iterations =   2.0

negative rho (up, down):   1.015E-04 9.067E-05

total cpu time spent up to now is   16.1 secs

total energy   =   -180.62688401 Ry
Harris-Foulkes estimate   =   -180.63312974 Ry
estimated scf accuracy   <   0.07140509 Ry

total magnetization   =   0.00 Bohr mag/cell
absolute magnetization   =   0.55 Bohr mag/cell

iteration # 3   ecut=   50.00 Ry   beta=0.40
Davidson diagonalization with overlap
ethr =   2.75E-04,   avg # of iterations =   2.0

negative rho (up, down):   1.023E-04 9.647E-05

total cpu time spent up to now is   19.2 secs

```
        total energy            =    -180.64606745 Ry
        Harris-Foulkes estimate =    -180.64692836 Ry
        estimated scf accuracy  <       0.05521308 Ry


        total magnetization     =       0.00 Bohr mag/cell
        absolute magnetization  =       0.48 Bohr mag/cell


        iteration #  4      ecut=    50.00 Ry      beta=0.40
        Davidson diagonalization with overlap
        ethr =   2.12E-04,  avg # of iterations =   1.5


        negative rho (up, down):   1.036E-04 1.047E-04


        total cpu time spent up to now is        23.3 secs
        total energy            =    -180.65774984 Ry
        Harris-Foulkes estimate =    -180.65248579 Ry
        estimated scf accuracy  <       0.00506783 Ry


        total magnetization     =       0.00 Bohr mag/cell
        absolute magnetization  =       0.32 Bohr mag/cell


     iteration #  5      ecut=    50.00 Ry      beta=0.40
        Davidson diagonalization with overlap
        ethr =   1.95E-05,  avg # of iterations =   2.1


        negative rho (up, down):   1.028E-04 1.041E-04


        total cpu time spent up to now is        27.9 secs


        total energy            =    -180.65900966 Ry
        Harris-Foulkes estimate =    -180.65880166 Ry
        estimated scf accuracy  <       0.00029637 Ry


        total magnetization     =       0.00 Bohr mag/cell
```

absolute magnetization   =   0.12 Bohr mag/cell

iteration # 6   ecut=   50.00 Ry   beta=0.40
Davidson diagonalization with overlap
ethr = 1.14E-06, avg # of iterations = 2.5

negative rho (up, down): 1.023E-04 1.033E-04

total cpu time spent up to now is   31.5 secs

total energy   =   -180.65921404 Ry
  Harris-Foulkes estimate   =   -180.65912686 Ry
  estimated scf accuracy   <   0.00006620 Ry

  total magnetization   =   0.00 Bohr mag/cell
  absolute magnetization   =   0.06 Bohr mag/cell

iteration # 7   ecut=   50.00 Ry   beta=0.40

  Davidson diagonalization with overlap
  ethr = 2.55E-07, avg # of iterations = 2.4

  negative rho (up, down): 1.024E-04 1.027E-04

  total cpu time spent up to now is   37.1 secs

  total energy   =   -180.65926406 Ry
  Harris-Foulkes estimate   =   -180.65924934 Ry
  estimated scf accuracy   <   0.00000699 Ry

  total magnetization   =   0.00 Bohr mag/cell
  absolute magnetization   =   0.03 Bohr mag/cell

iteration # 8   ecut=   50.00 Ry   beta=0.40
Davidson diagonalization with overlap
ethr = 2.69E-08, avg # of iterations = 3.0

negative rho (up, down): 1.025E-04 1.026E-04

total cpu time spent up to now is   41.4 secs

 total energy   =   -180.65927312 Ry
   Harris-Foulkes estimate   =   -180.65927273 Ry
   estimated scf accuracy   <   0.00000124 Ry

   total magnetization   =   0.00 Bohr mag/cell
   absolute magnetization   =   0.01 Bohr mag/cell

iteration # 9   ecut=   50.00 Ry   beta=0.40
   Davidson diagonalization with overlap
   ethr = 4.75E-09, avg # of iterations = 3.0
   negative rho (up, down): 1.026E-04 1.026E-04

   Magnetic moment per site:
   atom: 1   charge: 10.7495   magn: 0.0001   constr: 0.0000
   atom: 2   charge: 4.1520   magn: -0.0001   constr: 0.0000
   atom: 3   charge: 4.1520   magn: -0.0001   constr: 0.0000

   total cpu time spent up to now is   45.6 secs

   End of self-consistent calculation

   The Fermi energy is   0.4580 ev

total energy = -180.65927424 Ry

Harris-Foulkes estimate = -180.65927436 Ry

estimated scf accuracy < 0.00000027 Ry

The total energy is the sum of the following terms:

one-electron contribution = -963.55685944 Ry

hartree contribution = 482.37097304 Ry

xc contribution = -28.50920888 Ry

ewald contribution = 329.03585576 Ry

smearing contrib. (-TS) = -0.00003472 Ry

total magnetization = 0.00 Bohr mag/cell

absolute magnetization = 0.00 Bohr mag/cell

convergence has been achieved in 9 iterations

negative rho (up, down): 1.026E-04 1.026E-04

BFGS Geometry Optimization

bfgs converged in 1 scf cycles and 0 bfgs steps

(criteria: energy < 1.0E-04 Ry, force < 1.0E-03 Ry/Bohr)

End of BFGS Geometry Optimization

Final energy = -180.6592742443 Ry

Begin final coordinates

ATOMIC_POSITIONS (angstrom)

Mo   0.000000000   0.000000000   9.063556000

S   1.592033000   0.919161000 10.627113000

S   1.592033000   0.919161000   7.500000000

End final coordinates

CHAPTER 4

4.1. BAND STRUCTURE

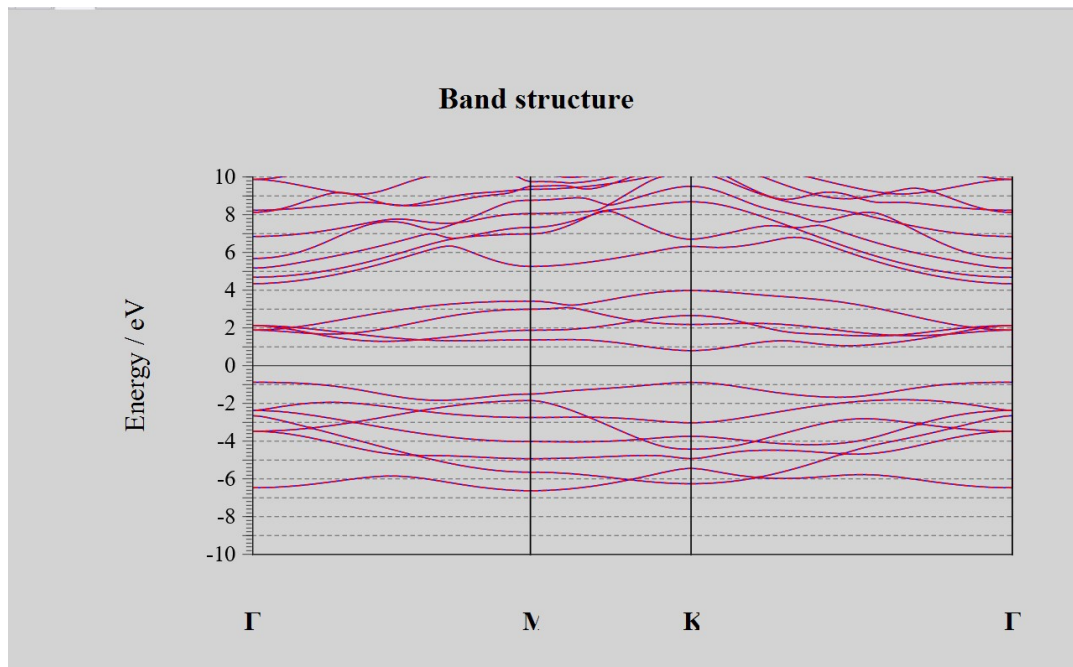The obtained band structure as an output is as shown,

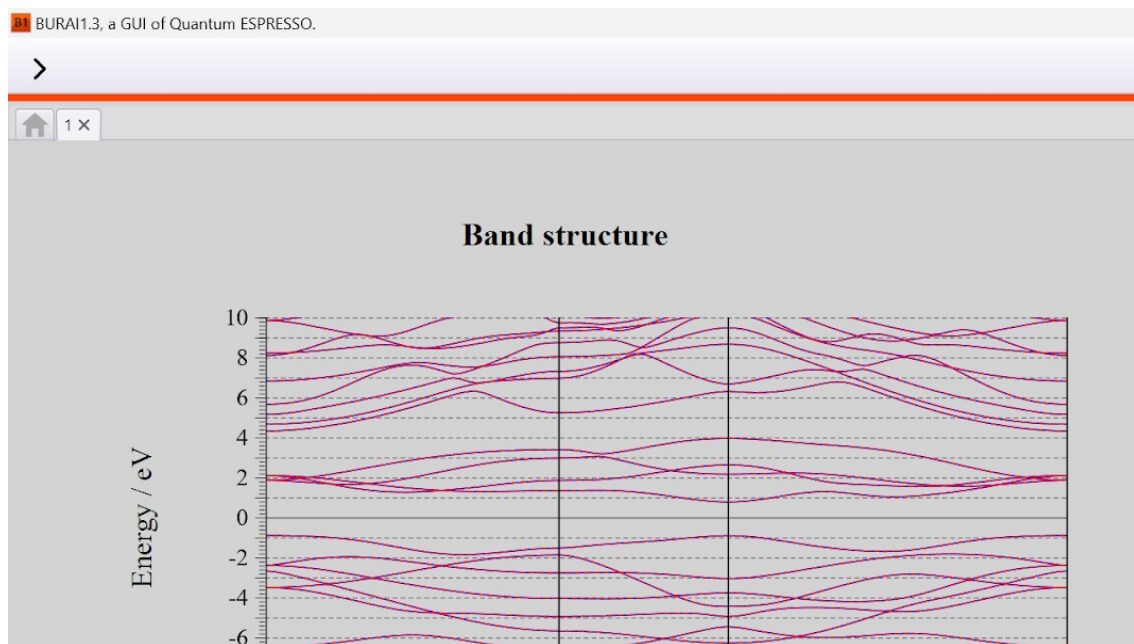Fig. The band structure of MoS_2 as obtained using quantum espresso.

Fig.Output view in the burai interface.

4.2. BANDGAP

The band structure of MoS_2 obtained using quantum espresso in the burai interface is a direct band gap from which the band gap energy can calculated as follows,
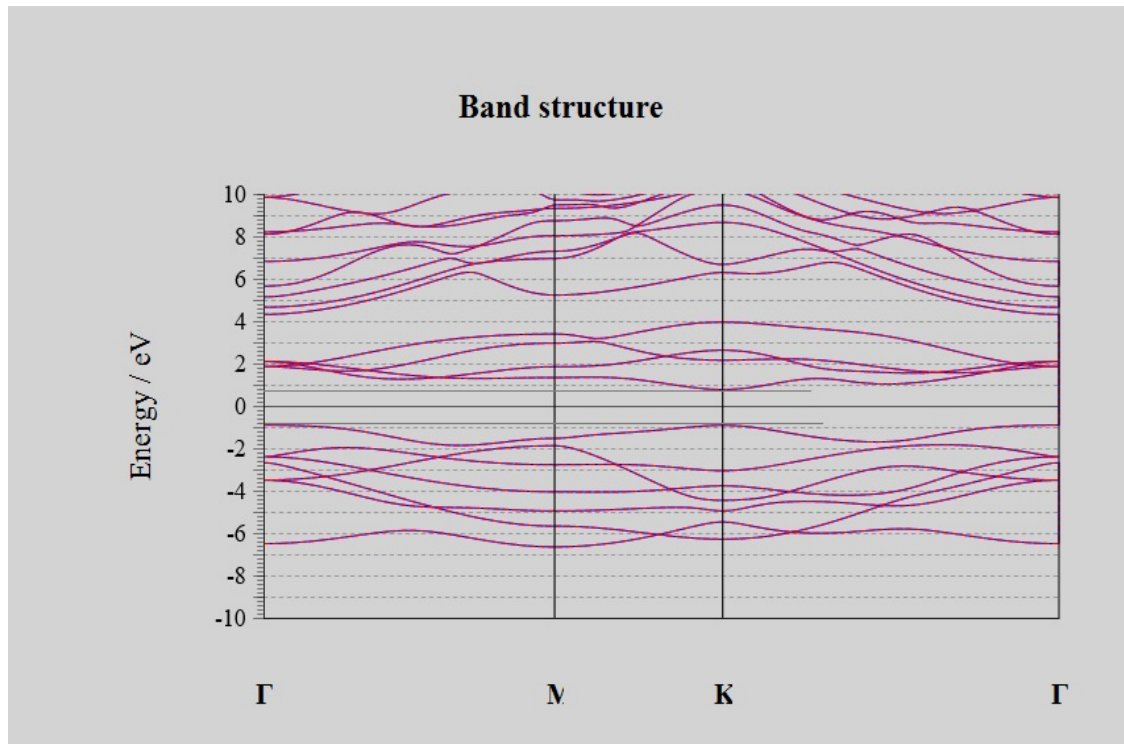

Fig.Band Structure Of MoS_2.

The band gap is given by the distance between the valence band and conduction band i.e. the energy difference between the top of valence band and bottom of conduction band. It is the energy required to promote an electron from the valence band to the conduction band. From the graph, the value of E_v is given by

$$E_v = -0.79 \text{ eV}$$

Similarly, the value of E_g is given by,

$$E_c = 0.8 \text{ eV}$$

The band gap energy is given by energy difference which is given by

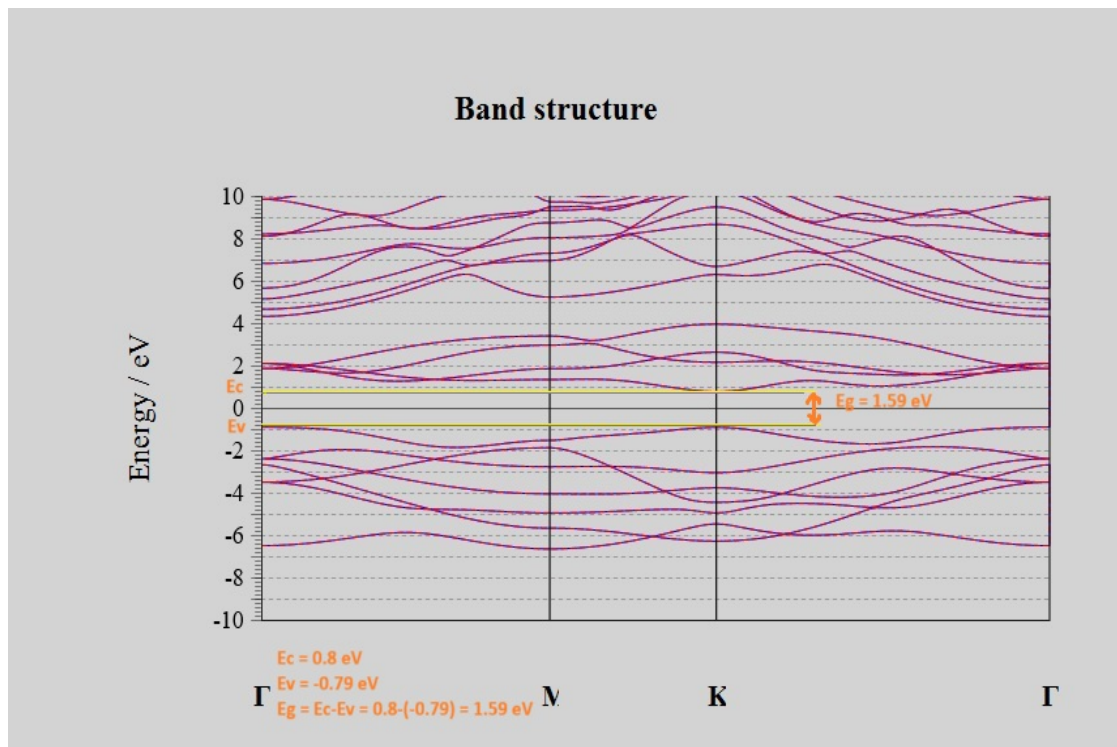$$E_g = E_c - E_v = 0.8 - (-0.79)$$
$$= 1.59 \text{ eV}$$

Fig.Calculation of band gap energy from the output band structure.

Therefore, from the graph the band gap energy of the 2D MoS_2 is found to be 1.59 eV.

4.3.COMPARISON WITH REPORTED VALUES

The bulk MoS_2 material is reported to have an indirect bandgap of 1.2 eV, whereas two-dimensional (2D) single-layer MoS_2 have a direct bandgap of 1.8 eV(1). From experimental observations and calculations, the bi layer MoS2 is found to have a bandgap energy of around 1.60 eV(2).
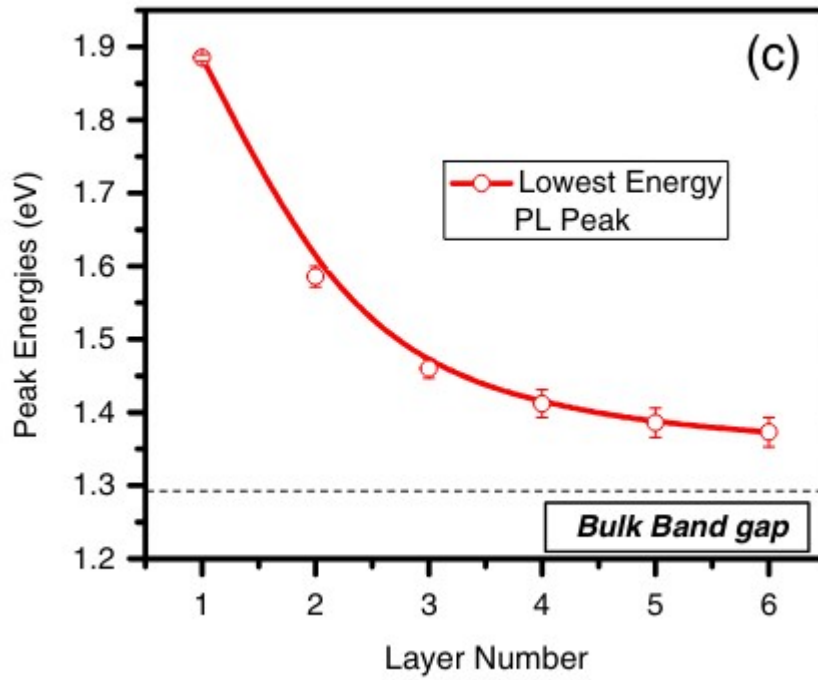
Fig.layer number vs peak energy graph

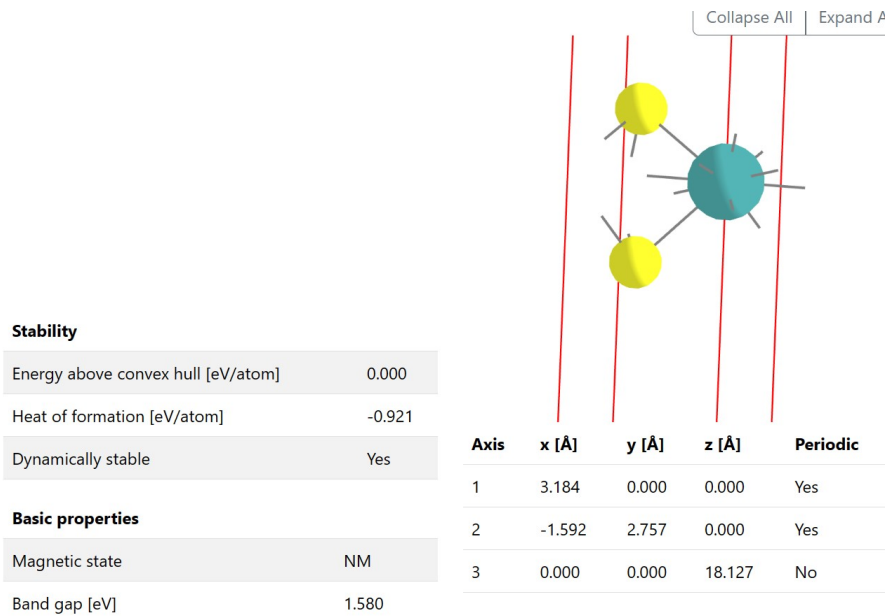The experimental band gap energy for the imported bi layer MoS_2 is given to be 1.58 eV.

Stability

Energy above convex hull [eV/atom]	0.000
Heat of formation [eV/atom]	-0.921
Dynamically stable	Yes

Basic properties

Magnetic state	NM
Band gap [eV]	1.580

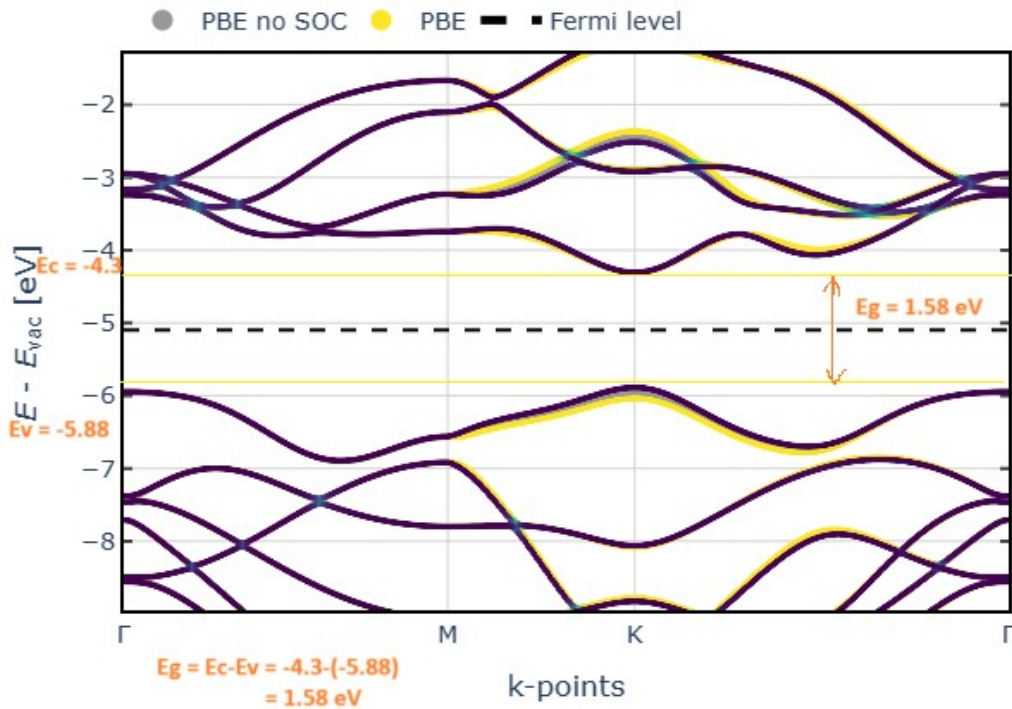| Axis	x [Å]	y [Å]	z [Å]	Periodic
1	3.184	0.000	0.000	Yes
2	-1.592	2.757	0.000	Yes
3	0.000	0.000	18.127	No

Fig.MoS_2 properties from C2DB.

Fig.Direct band structure and calculation of band gap energy of MoS_2 from C2DB.

From the above graph,

Ec = -4.3 eV

Ev = -5.88 eV

Hence the band gap energy is given by,

Eg = -4.3-(-5.88)

= 1.58 eV

On Comparison,

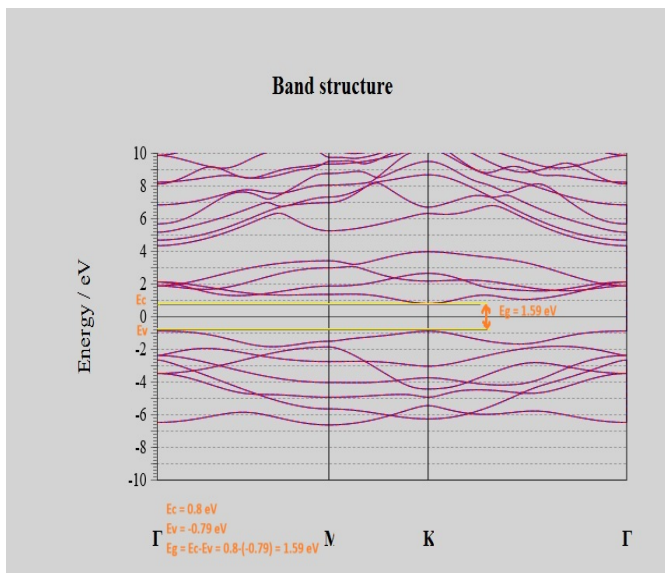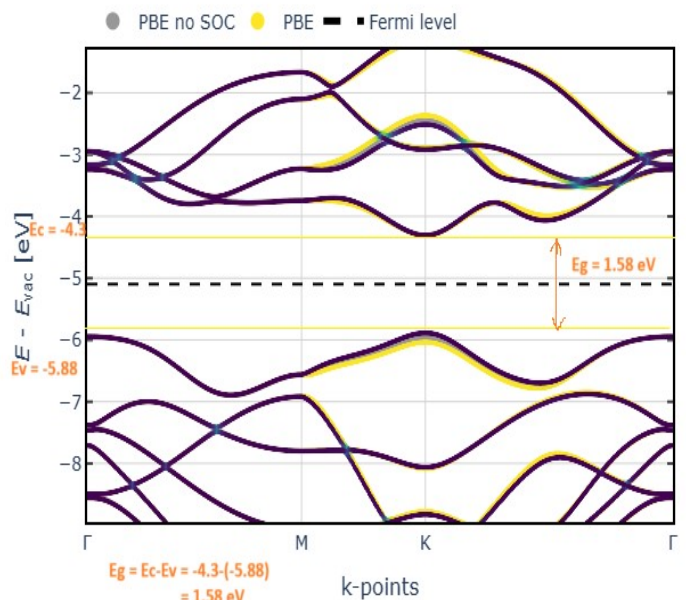Fig.Band gap energy from quantum espresso   Fig. Band gap energy from C2DB

The band gap energy of MoS_2 theoretically calculated using quantum espresso is found to be 1.59 eV. On considering the above mentioned experimental values and conclusion and hence on further comparison of the value so obtained theoretically and the value obtained experimentally, the band gap energy of MoS_2 can be optimized and interpreted using Quantum espresso.

Tabulating the experimental and calculated values of direct band gap energy of bi layer MoS_2 ,

STRUCTURE	BAND GAP ENERGY (eV)		REFERENCE OF EXPERIMENTAL VALUE
	EXPERIMENTAL	CALCULATED	
BI LAYER	1.58	1.59	1MoS2-1 (dtu.dk)
	1.60		Mak, K. F., Lee, C., Hone, J., Shan, J., & Heinz, T. F. (2010). Atomically ThinMoS2: A New Direct-Gap Semiconductor. Physical Review Letters, 105(13). doi:10.1103/physrevlett.105.136805 .
	1.68		Jiang, J. T., Xiu, S. L., Zheng, M. M., Jia, T. T., Liu, H. Y., Zhang, Y., & Chen, G. (2014). Indirect–direct bandgap transition and gap width tuning in bilayer MoS 2 superlattices. Chemical Physics Letters, 613, 74–79. doi:10.1016/j.cplett.2014.08.060

CHAPTER 5
CONCLUSION

Given the experimental data of a 2D material, the structural properties of a compound can be effectively interpreted theoretically. MoS_2 is a vastly explored and scientifically experimented structure in the current world due to its numerous advantages in optical, bio-medical and electronic applications. Band gaps depict the electrical properties of a material signifying whether the material is a metal, insulator or semiconductor. Band gaps refer to the energy difference between the highest occupied electronic state (valence band) and the lowest unoccupied electronic state (conduction band). They play a crucial role in determining the electrical behavior of materials.Materials with a large band gap are insulators, those with a small or no band gap are conductors (metals), and those with a moderate band gap are semiconductors.

MoS2, being a semiconductor, exhibits a finite band gap, making it useful in electronic devices where controlled electrical conductivity is required

Additionally, a material might become less reactive and more stable when a band gap is present.

Therefore, it can be concluded that the quantum espresso interface can be effective in generating and obtaining the band structure and thus the band gap Energy of 2D bilayer MoS_2.

REFERENCE

[1]

N. Thomas, S. Mathew, K.M. Nair, K. O'Dowd, P. Forouzandeh, A. Goswami, G. McGra naghan, S.C. Pillai**.** 2D MoS$_2$: structure, mechanisms, and photocatalytic applications. https://doi.org/10.1016/j.mtsust.2021.100073

[2]

Mak, K. F., Lee, C., Hone, J., Shan, J., & Heinz, T. F. (2010). Atomically ThinMoS2: A New Direct-Gap Semiconductor. Physical Review Letters, 105(13). doi:10.1103/physrevlett.105.136805.

[3]

Jiang, J. T., Xiu, S. L., Zheng, M. M., Jia, T. T., Liu, H. Y., Zhang, Y., & Chen, G. (2014). Indirect–direct bandgap transition and gap width tuning in bilayer MoS 2 superlattices. Chemical Physics Letters, 613, 74–79. doi:10.1016/j.cplett.2014.08.060.

[4]

Z. Y. Zhang,M. S. Si,Y. H. Wang,X. P. Gao,Dongchul Sung,Suklyun Hong,Junjie He Indirect-direct band gap transition through electric tuning in bilayer MoS$_2$ .J. Chem. Phys. 140, 174707 (2014).**https://doi.org/10.1063/1.4873406**

[5]

Computational 2d database (c2db). https://c2db.fysik.dtu.dk/